Enhanced ac conductivity below T_c in films of $YBa_2Cu_3O_{7-\delta}$

J. T. Moonen, L. J. Adriaanse, and H. B. Brom
Kamerlingh Onnes Laboratory, Leiden University, P.O. Box 9506, 2300 RA Leiden, The Netherlands

N. Y. Chen and D. van der Marel
Faculty of Applied Physics, Delft University of Technology, 2628 CJ Delft, The Netherlands

M. L. Horbach and W. van Saarloos
Institute Lorentz for Theoretical Physics, Leiden University, P.O. Box 9506, 2300 RA Leiden, The Netherlands
(Received 21 July 1992; revised manuscript received 25 January 1993)

In superconductors, close to the transition temperature, a peak in the real part of the conductivity $\sigma_1(T,\omega)$, can appear for several reasons. We show that even in the two-fluid model, a peak is present when there is a distribution of T_c's in the sample. A parasitic inductance modifies the features of a peak considerably, but in general does not generate a peak by itself. We illustrate this by four-contact-impedance measurements on thin (3000-Å) films of $YBa_2Cu_3O_{7-\delta}$ in the kHz regime.

I. INTRODUCTION

There have recently been experimental investigations of the behavior of the complex conductivity $\sigma=\sigma_1+i\sigma_2$ of the high-T_c superconductors as a function of temperature in several frequency regimes. These experiments have been performed with various motivations, as measurements at different frequencies may probe different physical phenomena. In Ref. 1, the conductivity was determined in the 100-GHz range in order to investigate the existence of a coherence peak, which is a prominent feature of BCS superconductors,[2] but which is absent in the NMR measurements on the high-T_c superconductors. Although a sharp enhancement of σ_1 was reported to occur slightly below T_c in these experiments, the interpretation[1] in terms of a coherence effect is questionable.[3–5] Another observation of a peak in the same frequency range[6] was interpreted[7] in terms of a temperature-dependent mixture of superconducting and normal grains in the sample. Measurements at higher frequencies [0.5–2 THz (Refs. 8 and 9) and 10 GHz (Ref. 15)] as a function of temperature, on the other hand, showed a very broad peak below T_c. This has been attributed to a rapid increase in the transport relaxation time below T_c, which is a natural feature of the marginal Fermi-liquid phenomenology or in fact any electronic pairing mechanism. Furthermore, peak observations in yet again other frequency ranges (1 kHz–20 MHz) have been seen as evidence for a Berezinskii-Kosterlitz-Thouless phase transition.[10–12] Finally, Olsson and Koch[13,4] attributed their peak in the range 20–450 MHz to a distribution to T_c's in the sample, which is an argument similar to the one given in Ref. 7. This idea was followed by Lunkenheimer *et al.*[14] and by Shibauchi *et al.*[15] to explain experiments in the range 10^5–10^8 Hz and at 10 GHz, respectively. The latter actually reports two peaks, an observation also made by Drotbohm *et al.*[16]

In Sec. II, a general condition for the appearance of a peak in σ_1 is given. We will concentrate on nonintrinsic properties that generate or modify a peak. By "nonintrinsic" we mean "not originating from the pure, single phase compound." Two special cases are discussed, one of them being the distribution of T_c's (caused by sample inhomogeneity) that was also considered in the above-mentioned Refs. 4, 7, and 13–15, the other being a parasitic inductance. These general considerations were motivated by peaks that we observed in four-contact ac measurements on $YBa_2Cu_3O_{7-\delta}$ (YBCO) films. We discuss the data in this paper. In Sec. III the experimental procedure is outlined and we discuss how the data were evaluated. In Sec. IV A the data above T_c are analyzed in terms of a Lawrence-Doniach model of fluctuations in a layered superconductor. The value of $T_c=89.2$ K obtained in the fit to this model is used in Sec. IV B for the analysis of the data below T_c. As mentioned above, the analysis illustrates how our data are influenced by the presence of a parasitic inductance.

II. NONINTRINSIC PEAKS

The relation between the impedance Z and the conductivity σ is given by

$$Z=R+iX=\frac{l}{bd\sigma} , \tag{1}$$

with $l\times b\times d$ the effective dimensions of the sample. So

$$\sigma_1\propto\frac{R}{R^2+X^2} \tag{2}$$

and

$$\sigma_2\propto\frac{-X}{R^2+X^2} . \tag{3}$$

A necessary condition for the presence of a peak in σ_1 is

$$\dot{\sigma}_1\propto-\dot{R}R^2-2RX\dot{X}+\dot{R}X^2=0 , \tag{4}$$

where the dots represent a derivative with respect to temperature. It is difficult to determine from Eq. (4) under which general conditions a peak in σ_1 will appear, but the trends become clear by considering some special cases.

First, in a two-fluid model, the conductivity below T_c is given by[17]

$$\sigma(\omega,T)=\sigma_1+i\sigma_2=\sigma_n(\omega,T)t^4-i\frac{1-t^4}{\omega\mu_0\lambda(0)^2}\ , \qquad (5)$$

where $t=T/T_c$, μ_0 is the free-space magnetic permeability, $\sigma_n(\omega,T)t^4$ is the conductivity contribution from the normal fraction (extrapolated from the normal state), and $\lambda(T)=\lambda(0)/\sqrt{1-t^4}$ is the penetration depth. The two-fluid model exhibits no peak for $T<T_c$, if the normal-state conductivity $\sigma_n(\omega,T)$ is a slowly varying function of T. The behavior of R and X is shown in Fig. 1(a) for $\sigma_n(\omega,T)\propto T^{-1}$. Now let us consider what will happen if there is a distribution of T_c's in the sample. For simplicity, we take a linear chain of domains A_i with critical temperatures T_{ci} and a distribution of T_c's $\rho(T_{ci})$. The total conductivity $\sigma(\omega,T)$ is then equal to the inverse of the sum of the impedances $Z_i(\omega,T)$. Each $Z_i(\omega,T)$ is individually determined by the two-fluid model. In this case, a peak in $\sigma_1(T)$ appears, due to the mixing of superfluid response in one area with normal response in another. In Fig. 2, we display σ_1 vs T for a Gaussian distribution with a full width at half height of 1 K at three frequencies. The height, position, and width of the peak depend on the specifics of the distribution and on frequency, the height varying as ω^{-1}. A clear ω^{-1} dependence resulting from sample inhomogeneity was observed by Lunkenheimer *et al.*[14] in Zn-doped YBCO films. Although the linear-chain two-fluid model is overly simplified, presumably a two-dimensional (2D) or three-dimensional (3D) effective medium or percolative model[18] will not change the trends qualitatively.

Second, we consider the influence of a parasitic L_p and C_p. We will discuss this influence in terms of the equivalent circuit of Fig. 3(a). Solving for X in Eq. (4), we obtain (with $\dot{R}\neq 0$)

$$X=R[\dot{X}/\dot{R}\pm\sqrt{1+(\dot{X}^2/\dot{R}^2)}]=A\pm B\ , \qquad (6)$$

with $B>|A|$, which means that $A-B$ is negative. The sign of $\dot{\sigma}_1$ as a function of X and $\dot{R}$ is drawn in Table I. In the two-fluid model, $\dot{\sigma}_1>0$, $\dot{R}>0$, and $X>0$ so that we are in a region where X is larger than $A+B$. Now let us consider the equivalent circuit with $C_p=0$. The reactance $X_p=\omega L_p$ will move X further away from the point $A+B$. Consequently no peak in σ_1 will be created by L_p. Adding a nonzero capacitance C_p only affects σ_2 and

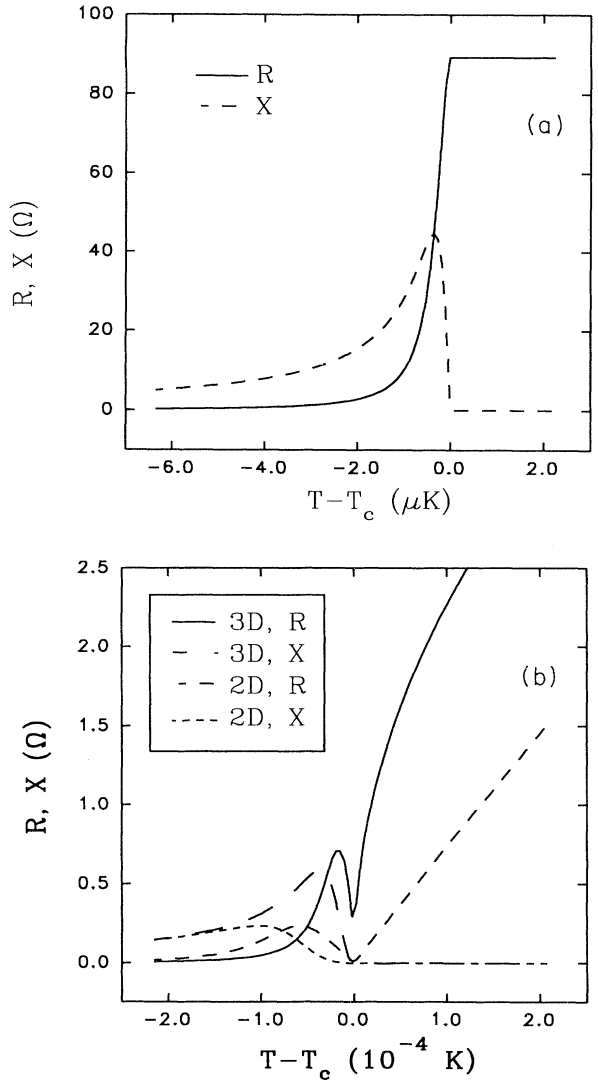

FIG. 1. R and X in the two-fluid model, (a) without and (b) with fluctuations in two and three dimensions (see the Appendix). Parameters: $T_c=89.2$ K, $\lambda_0=3000$ Å, $\omega/2\pi=60$ kHz, $R(100\ \text{K})=100\ \Omega$, and $\rho(100\ \text{K})=3\ \mu\Omega\,\text{m}$, $\sigma_n(\omega,T)\propto T^{-1}$, $\xi_0=5$ Å.

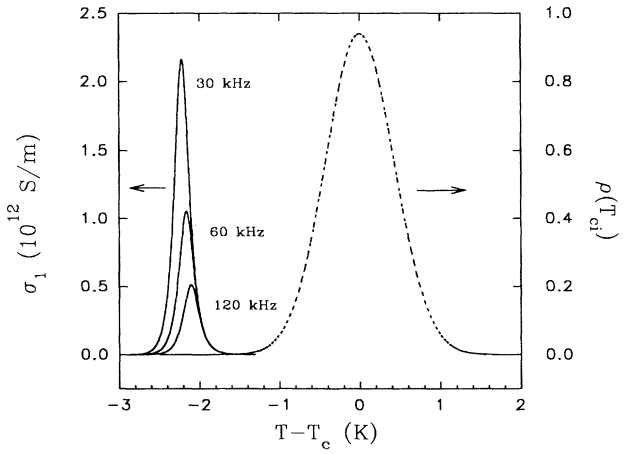

FIG. 2. Peak in the real part of the conductivity σ_1, obtained from the linear-chain, Gaussian broadened two-fluid model, at frequencies of 30, 60, and 120 kHz. The Gaussian distribution $\rho(T_{ci})$ with a full width at half height of 1 K is displayed in the figure also. Parameters are the same as in Fig. 1.

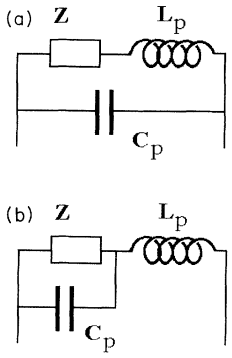

FIG. 3. Two equivalent circuits that can be used to evaluate impedance data, (a) is the circuit we used to evaluate our data. At low frequencies, circuit (b) gives the same results as circuit (a).

will not contribute to a peak either. So the circuit of Fig. 3(a) cannot generate a peak in σ_1 starting from the pure two-fluid model. However, if a peak is already present (whatever its origin) and if $\dot{R}>0$, L_p will shift the peak to a higher temperature (see Table I) and it will decrease its height [see Eq. (2)]. In the case of the BCS peak shown in the figure of Ref. 2, this effect is very drastic. A parasitic L_p of less than 10 pH shifts, narrows, and diminishes the peak substantially, whereas a larger value of L_p removes the peak structure completely. A parasitic X_p will also influence the frequency dependence of the height of a peak, making it look like ω^{-1}. In case fluctuations in the order parameter are added to the two-fluid model, $\dot{R}$ can become smaller than zero [see Fig. 1(b)]. From Table I it can be seen that then X_p will shift the fluctuation induced peak down in temperature.

By a similar line of reasoning, a residual R_p also greatly modifies a peak. Instead of solving for X, it is then better to solve Eq. (4) for R. We will not go into details, for in our experiment we seem not to be troubled by a residual resistance.

So we have shown that there are at least two scenarios in which a peak is either generated or greatly modified by extrinsic causes.

III. EXPERIMENTAL

Our data were obtained on epitaxial $YBa_2Cu_3O_{7-\delta}$ films in the kHz regime. Only data taken at 60 kHz are presented in the figures. The films with dimensions $d=3000$ Å, $b=8$ μm, and $l=80$ μm were prepared by a laser ablation technique on a $SrTiO_3$ substrate on the (001) surface.[19] Four terminal measurements were performed with a PAR lock-in amplifier (model 5210) with two-phase detection. No precautions were taken to expel the earth magnetic field.

TABLE I. Sign scheme for $\dot{\sigma}_1$ as a function of X and $\dot{R}$. The solutions of Eq. (4) when solved for X are $A-B$ and $A+B$.

	$X<A-B$	$A-B<X<A+B$	$X>A+B$
$\dot{R}>0$	$\dot{\sigma}_1>0$	$\dot{\sigma}_1<0$	$\dot{\sigma}_1>0$
$\dot{R}<0$	$\dot{\sigma}_1<0$	$\dot{\sigma}_1>0$	$\dot{\sigma}_1<0$

For the normal state, we estimate a skin depth of the order of 1 mm at 10^5 Hz, much larger than the film thickness of 3000 Å. The voltage V_{PAR} detected by the PAR is therefore proportional to Z and not to the so-called surface impedance $Z_s=(i\omega\mu_0/\sigma)^{1/2}$. For the superconducting state, we estimate that deviations from the proportionality relation $V_{PAR}\propto Z$ are at most 3% at 85 K, becoming larger at lower temperatures as the penetration depth decreases. For the present results, deviations from the proportionality relation can be neglected. At higher frequencies and lower temperatures, however, one should take this deviation into account.[20]

As shown in Fig. 4, where we present the raw data, the resistance $R(T)$ that we measure starts to increase at around 88 K, becoming linear at high temperatures. The nonzero impedance $X(T)$ does not change with temperature from 80 K to just below T_c (89.2 K at the midpoint of the transition). It rises to a maximum near T_c, while it drops below zero above T_c. The constant X value below T_c is found to be linear with frequency, as expected for a superconductor.

The drawn line through the data points is a fit to a model, which is further explained in Sec. IV A. It is based on the two-fluid model for the superconducting state, a normal-state resistivity linear in T and a fluctuation contribution. It also includes an evaluation of $Z(T)$ and its frequency dependence by means of the equivalent circuit shown in Fig. 3(a), similar to the analysis of Lunkenheimer *et al.*,[14] who used the circuit of Fig. 3(b). We assume that above T_c the intrinsic X without fluctuations is zero, like in a normal metal at these low frequencies. A parasitic capacitance $C_p\approx 700$ pF, arising from coaxial cables, modifies Z above T_c, where the intrinsic R is large. When R becomes of the order of a few ohms, the effect of the capacitance can be neglected. The equivalent network then contains only an inductance L_p of approximately 0.2 μH. This value, measured with the sample replaced by a thin ($\ll$skin depth) copper wire, is temperature independent up to ambient temperature. It originates from the mutual inductance between the current and voltage leads. Because of inevitable modifications in the setup when replacing the sample, the inaccuracy in L_p was about 20%. This low accuracy, together with the large value of L_p, made an experimental determination of the film properties below T_c impossible.

IV. ANALYSIS OF DATA

A. Analysis of the data above T_c

Above T_c, fluctuations can alter the resistance in a drastic manner. Lawrence and Doniach[21] have derived an expression for the fluctuation enhanced dc conductivity in a layered superconductor:

$$(\delta\sigma)^{-1}=\frac{C16\hbar d\epsilon}{e^2}\left[1+\left[\frac{2\xi_{01}}{d}\right]^2\epsilon^{-1}\right]^{1/2} \quad (7)$$

or

$$(\delta\sigma)^{-1}=\left[\left[\frac{1}{\delta\sigma_{2D}}\right]^2+\left[\frac{1}{\delta\sigma_{3D}}\right]^2\right]^{1/2}, \quad (8)$$

with C a constant of the order unity, d the interlayer distance, ϵ the reduced temperature $\ln(T/T_c)$ (Ref. 22) [which reduces near T_c to $(T-T_c)/T_c$], $\xi_{0\perp}$ the zero-temperature coherence length perpendicular to the layers and $\delta\sigma=1/\rho-1/\rho_n$. The temperature determines the nature of the fluctuations. For T near T_c, where $\xi_\perp(T)=\xi_{0\perp}\epsilon^{-1/2}$ is larger than d, the second term under the square root in Eqs. (7) and (8) dominates and three-dimensional behavior is recovered $[(\delta\sigma)^{-1} \propto (T-T_c)^{1/2}]$. Away from T_c the two-dimensional fluctuations are more important $[(\delta\sigma)^{-1}\propto(T-T_c)]$.

The dc Lawrence-Doniach expression remains valid for $R(T,\omega)$ at nonzero but small frequencies if $|T-T_c|$ is sufficiently large. In our case, at frequencies of about 100 kHz, deviations from the limiting dc behavior can be expected at most within a few μK of T_c. However, $X(T,\omega)$ is only defined for nonzero frequencies, and the frequency-dependent expression should be used (see the Appendix). We used the analog of Eq. (8) to obtain the Lawrence-Doniach equivalent of $\delta\sigma_2$. Above T_c, the modification of the intrinsic X due to fluctuations is very small.

In the expression for $\delta\sigma$, the normal-state resistivity ρ_n should be determined self-consistently, i.e., by taking both a and b in the empirical parametric formula $\rho_n=aT+b$ as fit parameters. The procedure to extrapolate ρ_n from the high-temperature region is not unambiguous, because fluctuations can have influence on the resistivity up to very high temperatures.[23,24] If we assume that the Lawrence-Doniach expression remains valid up to 200 K, the absolute deviation from an idealized normal-state resistivity $\rho_n=aT$ caused by fluctuations is even larger at 200 K than at 100 K. This means that the slope obtained from a fit of a high-temperature part of the total resistivity is smaller than that of the normal-state resistivity a. For the analysis of our data, we determined the normal-state resistance by fitting the high-temperature (>200 K) part of the resistance with the expression $R_n=AT+B$. We then adjusted A (with a few %) and B (with a few Ω's) so that the Lawrence-Doniach expression gave a reasonable fit, see Fig. 4.

In Fig. 5 we plot R and X vs T near T_c and the best fit with the Lawrence-Doniach formula. Note that the presence of the parasitic capacitance C_p reflects the large R fluctuations in the uncorrected X and masks the small fluctuations in the intrinsic X.

In the fit with Eq. (7) a coherence length $\xi_{0\perp}=2.1$ Å, a CuO_2 interlayer distance $d=11.7$ Å and $T_c=89.2$ K are used. This means that the 2D–3D crossover temperature is at about 100 K. The optimal value of C is about twice the theoretical value. A similar observation was made by other groups.[25–27] A best fit with $C=1$ gave (keeping d and T_c fixed) $\xi_{0\perp}=5$ Å, close to the value found by Semba, Ishii, and Matsuda.[28] The parameters are indeed found to be frequency independent, as assumed above.

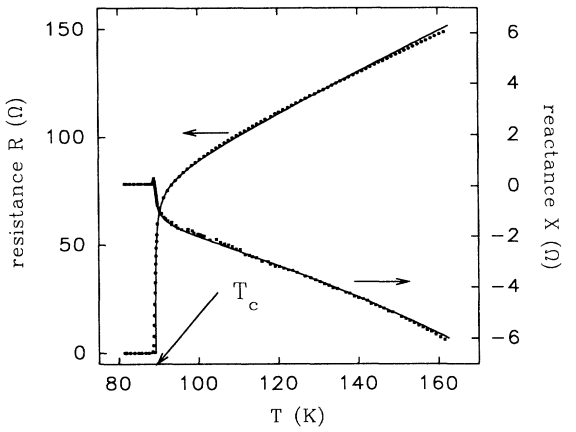

FIG. 4. A typical result for the T dependence of the resistance R at a frequency of 60 kHz. The three samples we measured gave essentially the same results. Drawn curves are a fit with a model explained in the text.

B. Analysis of the data close to T_c and below

As can be seen from Fig. 5, there is a small peak in X and a temperature-dependent nonzero resistance R below T_c. This resistance is too large to be attributed to fluctuations in the magnitude of the order parameter. Several possibilities remain: The transition could be (extra) broadened due to a distribution of T_c's, the ambient magnetic field (which introduces free vortices in the sample if it is larger than H_{c1}), or motion of unbound vortex-antivortex pairs as considered in the Berezinskii-Kosterlitz-Thouless (BKT) theory, which may be applicable due to the granular structure of the film or the (quasi-) 2D nature of the superconductor. Previously, high-resistance films of low-temperature superconductors,[29] as well as thin films and single crystals of high-T_c superconductors,[30–32] have shown the relevant features predicted by the BKT theory. It is very easy to obtain an excellent

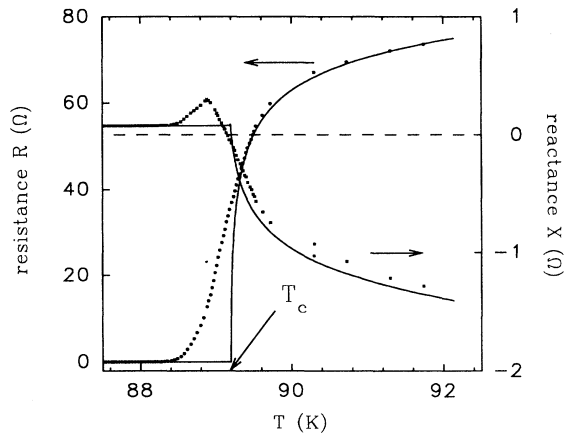

FIG. 5. Data and Lawrence-Doniach fit (drawn curve) of the data at 60 kHz close to T_c.

fit to the data if we add to our fitting model a linear-chain Gaussian distribution (with a full width at half height of 1 K) of T_c's. Although a small spread in oxygen concentration could account for the distribution of T_c's,[33] we do not consider this a satisfying description for the reason mentioned in Sec. II. The question about the precise origin of the broadening of the transition will be left open.

Because an accurate experimental determination of L_p was impossible, we determined the value of L_p indirectly by using the two-fluid model for the superconducting state [Eq. (5)], with the value of T_c taken from a fit of the data to the Lawrence-Doniach model and λ_0 of the order of several thousand Å. This procedure corresponds to subtracting a value of X_p that is very close to the measured constant X at low T (about 0.204 μH). Therefore, only a rough estimate can be made for the penetration depth λ_0 of the film. As already mentioned, the fitting curves of Figs. 4 and 5 were obtained with the aid of this procedure.

To illustrate the effect that a parasitic inductance has, we display in Fig. 6 σ_1 as a function of T below T_c, obtained from one single data set at 60 kHz but with different corrections $X_p=\omega L_p$ applied. The trend is clear: Subtracting a value which is closer to the constant X value below T_c (corresponding to about 0.204 μH) gives a higher peak at a lower temperature. When fully accounting for the parasitic inductance, the upper most curve is obtained. No clear peak feature is visible. In contrast, is we subtract a value of X_p that is obviously too small, namely $X_p/\omega=0.1$ μH (half the value measured), a clear peak is observable. We are then in the situation

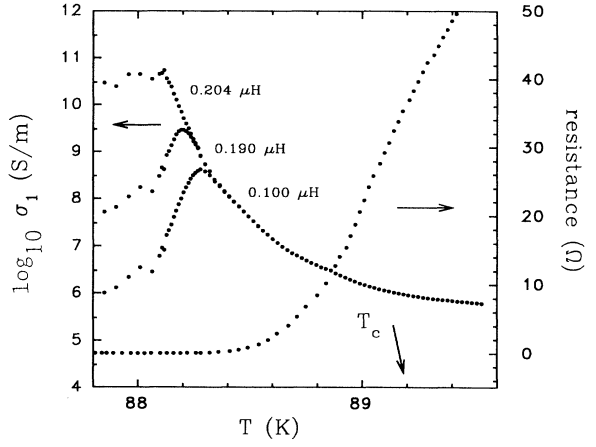

FIG. 6. Left axis: σ_1 as a function of T at 60 kHz. The three curves were obtained by subtracting different values of L_p, which are displayed next to the curves. The upper curve, which shows no clear peak feature because of the experimental noise, is obtained by subtracting an L_p value which is estimated by using the two-fluid model for X with $\lambda_0\sim3000$ Å. The lower curve is artificial in the sense that the subtracted value of L_p is obviously too small, a conclusion drawn from both the two-fluid model and experimental determination of L_p. The middle curve is shown to illustrate the trend mentioned in Sec. IV B. Right axis: the resistance as a function of temperature.

that R crosses a temperature-independent X_p. From Eqs. (2) and (4) it is evident that there is an (artificial) peak at the crossing point. This artificial peak resembles to some extent the peak that can arise from at least two phenomena. The similarities (and dissimilarities) are discussed in the following.

The anisotropy of YBCO is rather modest, leading to three-dimensional behavior within several degrees around T_c, as proved by the Lawrence-Doniach analysis of Sec. IV A. The expected height of the 3D-fluctuation peak for YBCO (see the Appendix) is of the same order of magnitude as the height of the artificial peak generated by L_p. Although the theoretical fluctuation peak is much narrower and occurs right at T_c, a distribution of T_c's could account for a broadening of the peak and the shift to lower temperature. For 3D fluctuations, the peak height should behave as $\omega^{-1/2}$. In contrast, the artificial peak has a ω^{-1} dependence, which is explained with the arguments given in Sec. II. The ω^{-1} dependence can only be found in the case that fluctuations are of 2D nature, like in for example $Bi_2Sr_2CaCu_2O_8$.[3]

The artificial peak resembles even more the peak predicted in the dynamic extension of the Berezinskii-Kosterlitz-Thouless theory.[34,35] It is predicted that the height varies approximately as ω^{-1} and that the location is at a temperature between the vortex unbinding temperature $T_{\rm BKT}$ and the superconducting mean field $T_c^{\rm MF}$, which lies slightly above $T_{\rm BKT}$. The position of our artificial peak (in the foot of the resistive tail), as well as the variation of its height with frequency, agree with these predictions. Because $YBa_2Cu_3O_{7-\delta}$ has predominantly 3D character near T_c, we do not expect a true Berezinskii-Kosterlitz-Thouless transition in our relatively thick films. Paracchini and Romanó[32] have found that their current-voltage data on bulk single crystals of YBCO are well described by a quasi-2D extension[36] of the Berezinskii-Kosterlitz-Thouless theory, thereby incorporating the effect of coupling between the layers on a transition within the layers. In this quasi-2D picture, the jump in σ_2 at $T_{\rm BKT}$ (as predicted by the 2D theory) is smeared out over a substantial temperature range and there is a nonohmic resistance between $T_{\rm BKT}$ and $T_c^{\rm MF}$. The BKT peak will then be broadened accordingly.

It is obvious that the above models do not describe the artificial peak, because we explicitly did not remove all parasitic effects and we have shown that these severely affect the data, both theoretically and experimentally. In general, because of the similarities between artificial and theoretical peaks it may be difficult to identify a clean intrinsic peak unambiguously.

V. CONCLUSION

We stated, in terms of the impedance Z, the condition for the appearance of a peak in the real part of the conductivity σ_1. Two examples were given of conditions that induce a nonintrinsic peak or modify an intrinsic peak: a distribution of T_c's and a parasitic inductance. Using experiments on thin films of $YBa_2Cu_3O_{7-\delta}$ in the kHz regime, we illustrate that the latter mechanism hinders an experimental observation of an intrinsic peak in σ_1. The

peak that appears when not fully accounting for the parasitic inductance, shows similarities to peaks predicted in fluctuation theory and the Berezinskii-Kosterlitz-Thouless theory.

ACKNOWLEDGMENTS

It is a pleasure to thank L. J. de Jongh, J. C. Martinez, and D. van der Putten for stimulating discussions. This work is part of the research program of the Leiden Materials Science Center and is supported by the Foundation of Fundamental Research on Matter (FOM), which is sponsored by the Netherlands Organization for the Advancement of Pure Research (NWO).

APPENDIX: THE FLUCTUATION CONTRIBUTION TO σ_1

The real part

The fluctuation contribution to σ_1, as calculated for thin films by Aslamasov and Larkin,[37] was generalized by Schmidt[38,39] for finite frequencies. The result for films with a thickness that is of the order of the coherence length ξ_0, written in a scaling form, is[40]

$$\delta\sigma_1(\omega)=\frac{1}{\omega}F\left[\frac{\omega}{\epsilon}\right], \tag{A1}$$

while for a bulk sample

$$\delta\sigma_1(\omega)=\frac{1}{\sqrt{\omega}}G\left[\frac{\omega}{\epsilon}\right]. \tag{A2}$$

with $\epsilon\equiv|T-T_c|$. For small values of x, $F(x)\sim x$ and $G(x)\sim\sqrt{x}$. Both functions increase monotonously to a constant at large values of x. This leads to a finite peak in $\delta\sigma_1$ at T_c. It follows from the properties of the functions F and G that the height of the peak is proportional to $1/\omega$ for films and to $1/\sqrt{\omega}$ for bulk samples. For $\omega\to 0$ the dc result is obtained, which means that $\delta\sigma_1\to\infty$ if $T\to T_c$. The 3D regime extends to several K away from T_c in $YBa_2Cu_3O_{7-\delta}$ (Sec. II A). Using the 3D-fluctuation result, the height of the narrow peak in $\delta\sigma_1$ at a frequency of 60 kHz is about 7×10^8 (S/m), while $\sigma_{1n}\sim4\times10^5$ (S/m), which means that the ratio $\sigma_1/\sigma_{1n}\sim10^3$ at T_c. The width ΔT of the peak at half of its height is obtained from the requirement that G reaches half of its limiting value at T_c, which occurs when $\tau_{GL}\omega/2=(\omega\hbar\pi)/(8k_B\Delta T)\sim1$. This implies that at a frequency of about 60 GHz the peak width ΔT is of the order of 1 K, while at 60 kHz the width is about 1 μK. Likewise, large deviations from the limiting dc behavior above T_c can be expected only when $\tau_{GL}\omega>1$. Note, however, that for the high-T_c materials the critical regime in which deviations from the Ginzburg-Landau behavior are noticable, is expected to be larger than 1 μK.

The imaginary part

An expression for the imaginary part of the fluctuation contribution to σ below T_c can be found in Ref. 39. To obtain the imaginary part of the fluctuation conductivity above T_c, we note that the real part is given by Schmidt[38] in reduced units ($k_B=\hbar=c=1$):

$$\mathrm{Re}\sigma_{ij}(\omega,K)=\left[\frac{2e}{m}\right]^2\frac{T_c}{V}\sum_q\frac{q_iq_j}{[\alpha+(1/2m)(q-(K/2))][\alpha+(1/2m)(q+(K/2))]}\frac{\Gamma_{q+(K/2)}+\Gamma_{q-(K/2)}}{[\omega^2+(\Gamma_{q+(K/2)}+\Gamma_{q-(K/2)})^2]}, \tag{A3}$$

with $i,j\equiv x,y,z$, $\alpha\propto\epsilon\equiv(T-T_c)/T_c$ and $\Gamma_q=8T_c\epsilon(\pi\alpha)^{-1}(\alpha+q^2/2m)$. Because σ has no poles in the upper half plane, we can write the complex σ as

$$\sigma_{ij}(\omega,K)=\left[\frac{2e}{m}\right]^2\frac{T_c}{V}\sum_q\frac{q_iq_j}{[\alpha+(1/2m)(q-(K/2))^2][\alpha+(1/2m)(q+(K/2))^2]}\frac{1}{[-i\omega+\Gamma_{q-(K/2)}+\Gamma_{q+(K/2)}]}. \tag{A4}$$

The imaginary part then becomes

$$\mathrm{Im}\sigma_{ij}(\omega,K)=\left[\frac{2e}{m}\right]^2\frac{T_c}{V}\sum_q\frac{q_iq_j}{[\alpha+(1/2m)(q-(K/2))^2][\alpha+(1/2m)(q+(K/2))^2]}\frac{\omega}{\{\omega^2+[\Gamma_{q+(K/2)}+\Gamma_{q-(K/2)}]^2\}}. \tag{A5}$$

For $K=0$:

$$\mathrm{Im}\sigma_{ij}(\omega)=\left[\frac{2e}{m}\right]^2\frac{T_c}{V}\sum_q\frac{q_iq_j}{[\alpha+(q^2/2m)]^2}\frac{\omega}{(\omega^2+4\Gamma_q^2)}. \tag{A6}$$

For σ diagonal and with the substitutions $\tilde{\omega}\equiv\pi\omega/(16T_c\epsilon)$, $\tilde{q}\equiv q(2m\alpha)^{-1/2}=q\xi$ (with ξ the temperature-dependent Ginzburg-Landau coherence length) and $x\equiv\tilde{q}^2$, we obtain for $D=2$ ($T>T_c$):

$$\mathrm{Im}\sigma=\frac{e^2}{8d\epsilon\tilde{\omega}}\int_0^\infty dx\left[\frac{x}{(1+x)^2}-\frac{x}{\tilde{\omega}^2+(1+x)^2}\right]=\frac{e^2}{8d\epsilon\tilde{\omega}}\left[-1+\frac{1}{2}\ln(1+\tilde{\omega}^2)+\frac{\pi}{2\tilde{\omega}}-\frac{1}{\tilde{\omega}}\arctan\frac{1}{\tilde{\omega}}\right], \tag{A7}$$

with d the thickness of the layer.

For $D=3$ and $T>T_c$ the expression is

$$\begin{aligned}\mathrm{Im}\sigma&=\frac{\tilde{\omega}e^2}{6\pi\epsilon\xi}\int_0^\infty d\tilde{q}\left[\frac{\tilde{q}^4}{(1+\tilde{q}^2)^2[\tilde{\omega}^2+(1+\tilde{q}^2)^2]}\right]\\&=\frac{\tilde{\omega}e^2}{6\pi\epsilon\xi}\int_0^\infty d\tilde{q}\left[\frac{\tilde{\omega}^2+1}{\tilde{\omega}[\tilde{\omega}^2+(1+\tilde{q}^2)^2]}+\frac{2\tilde{q}^2}{\tilde{\omega}^2[\tilde{\omega}^2+(1+\tilde{q}^2)^2]}-\frac{1}{\tilde{\omega}^2(1+\tilde{q}^2)}+\frac{1}{\tilde{\omega}^2(1+\tilde{q}^2)^2}\right]\\&=\frac{e^2}{6\epsilon\xi\tilde{\omega}}\left[-\frac{3}{4}+\frac{(\tilde{\omega}+1)^{3/4}}{2\tilde{\omega}}\sin\left[\frac{\arctan(\tilde{\omega})}{2}\right]+\frac{(\tilde{\omega}^2+1)^{1/4}}{\tilde{\omega}}\sin\left[\frac{\arctan(\tilde{\omega})}{2}\right]\right].\end{aligned} \tag{A8}$$

For conversion to S.I. units, in both expressions $\hbar$ should be added to the denominator of the prefactor and $\tilde{\omega}$ should be replaced by $\pi\hbar\omega/(16k_BT_c\epsilon)$.

[1]K. Holczer, L. Forro, L. Mihály, and G. Grüner, Phys. Rev. Lett. **67**, 152 (1991).

[2]M. Tinkham, *Introduction to Superconductivity* (Krieger, Malabar, 1975), p. 296 (1980 edition).

[3]M. L. Horbach, W. van Saarloos, and D. A. Huse, Phys. Rev. Lett. **67**, 3464 (1991); M. L. Horbach and W. van Saarloos, Phys. Rev. B **46**, 432 (1992).

[4]H. K. Olsson and R. H. Koch, Phys. Rev. Lett. **68**, 2406 (1992).

[5]O. Klein, K. Holczer, and G. Grüner, Phys. Rev. Lett. **68**, 2407 (1992).

[6]P. H. Kobrin, J. T. Cheung, W. W. Ho, N. Glass, J. Lopez, I. S. Gergis, R. E. DeWames, and W. F. Hall, Physica C **176**, 121 (1991).

[7]N. E. Glass and W. F. Hall, Phys. Rev. B **44**, 4495 (1991).

[8]M. C. Nuss, P. M. Mankiewich, M. L. O'Malley, E. H. Westerwick, and P. B. Littlewood, Phys. Rev. Lett. **66**, 3305 (1991).

[9]E. J. Nicol and J. P. Carbotte, Phys. Rev. B **44**, 7741 (1991).

[10]V. A. Gasparov, Physica C **178**, 449 (1991).

[11]P. K. Srivastava, P. Debely, H. E. Hintermann, C. Leemann, J. Weber, O. Caccivio, P. Martinoli, and H. R. Ott, Physica C **153-155**, 1443 (1988).

[12]A. T. Fiory, A. F. Hebard, P. M. Mankiewich, and R. E. Howard, Phys. Rev. Lett. **61**, 1419 (1988).

[13]H. K. Olsson and R. H. Koch, Physica C **185-189**, 1847 (1991).

[14]P. Lunkenheimer, A. Loidl, C. Tomé-Rosa, and H. Adrian, Physica C **201**, 13 (1992).

[15]T. Shibauchi, A. Maeda, H. Kitano, T. Honda, and K. Uchinokura, Physica C **203**, 315 (1992).

[16]P. Drotbohm, G. J. Russell, A. Bailey, G. Alvarez, and K. N. R. Taylor, Physica C **195**, 28 (1992).

[17]M. Tinkham, *Superconductivity* (Gordon and Breach, New York, 1965).

[18]G. Deutscher, O. Entin-Wohlman, S. Fishman, and Y. Shapira, Phys. Rev. B **21**, 5041 (1980).

[19]N. Y. Chen, K. van Dijk, L. W. Lander, H. M. Appelboom, D. van der Marel, P. Hadley, and J. E. Mooij, in *High-T_c Superconductor Thin Films,* edited by L. Correra (Elsevier Science, Amsterdam, 1992).

[20]M. S. Raven, E. E. Inameti, B. G. Murray, and Y. M. Wan, Physica C **178**, 275 (1991).

[21]W. E. Lawrence and S. Doniach, in *Proceedings of the LT-12,* Kyoto, Japan, 1970, edited by Eizo Kanda (Keigaku, Tokyo, 1971), p. 361.

[22]See, e.g., T. A. Friedmann, J. P. Rice, J. Giapintzakis, and D. M. Ginsberg, Phys. Rev. B **39**, 4258 (1989).

[23]R. E. Walstedt, R. F. Bell, L. F. Schneemeyer, J. V. Waszczak, and G. P. Espinosa, Phys. Rev. B **45**, 8074 (1992).

[24]Y. Iye, in *Physical Properties of High-Temperature Superconductors,* edited by D. M. Ginsberg (World Scientific, Singapore, 1992), p. 58.

[25]S. J. Hagen, Z. Z. Wang, and N. P. Ong, Phys. Rev. B **38**, 7137 (1988).

[26]D. H. Kim, A. M. Goldman, J. H. Kang, K. E. Gray, and R. T. Kampwirth, Phys. Rev. B **39**, 12 275 (1989).

[27]B. Oh, K. Char, A. D. Kent, M. Naito, M. R. Beasley, T. H. Geballe, R. H. Hammond, A. Kapitulnik, and J. M. Graybeal, Phys. Rev. B **37**, 7861 (1988).

[28]K. Semba, T. Ishii, and A. Matsuda, Phys. Rev. Lett. **67**, 769 (1991).

[29]A. F. Hebard and A. T. Fiory, Phys. Rev. Lett. **44**, 291 (1980); A. T. Fiory and A. F. Hebard, Phys. Rev. B **28**, 5075 (1983).

[30]P. K. Srivastava, P. Debely, H. E. Hintermann, C. Leemann, J. Weber, O. Caccivio, P. Martinoli, and H. R. Ott, Physica C **153-155**, 1443 (1988); Ref. 12.

[31]S. Martin, A. T. Fiory, R. M. Fleming, G. P. Espinosa, and A. S. Cooper, Phys. Rev. Lett. **62**, 677 (1989).

[32]C. Paracchini and L. Romanó, Physica C **184**, 29 (1991).

[33]H. F. Poulsen, N. H. Andersen, J. V. Andersen, H. Bohr, and O. G. Mouritsen, Nature (London), **349**, 594 (1991).

[34]V. Ambegaokar, B. I. Halperin, D. R. Nelson, and E. D. Siggia, Phys. Rev. Lett. **40**, 783 (1978).

[35]B. I. Halperin and D. R. Nelson, J. Low Temp. Phys. **36**, 599 (1979).

[36]S. Hikami and T. Tsuneto, Prog. Theor. Phys. **63**, 387 (1980).

[37]L. G. Aslamasov and A. I. Larkin, Phys. Lett. **26A**, 238 (1968).

[38]H. Schmidt, Z. Phys. **216**, 336 (1968).

[39]H. Schmidt, Z. Phys. **232**, 443 (1970).

[40]The general scaling form is $\sigma(\omega)=(1/\omega)F(\omega\epsilon^{-\nu z})$, see D. S. Fisher, M. P. A. Fisher, and D. A. Huse, Phys. Rev. B **43**, 130 (1991). Expression (A1) is obtained using the mean-field exponents. Similar for expression (A2).